

## Supporting information

### **Metal-free Bi-functional Cooperative catalysis: Amine and quaternary amine-functionalized dendritic fibrous nanosilica as heterogeneous catalysts for Henry reaction and CO<sub>2</sub> conversion†**

Sanjay Yadav,<sup>\*ac‡</sup> Hanuman G. Kachgunde,<sup>bc‡</sup> Nishu Choudhary,<sup>ac</sup> Gopal H. Wanole,<sup>bc</sup> Krishnan Ravi,<sup>\*bc</sup> Ankush V. Biradar,<sup>\*bc</sup> and Alok Ranjan Paital<sup>\*ac</sup>

<sup>a</sup>*Salt and Marine Chemicals Division, CSIR-Central Salt & Marine Chemicals Research Institute, G.B. Marg, Bhavnagar-364002, Gujarat, India.*

*E-mail: [arpaital@csmcri.res.in](mailto:arpaital@csmcri.res.in); [sychem00700@gmail.com](mailto:sychem00700@gmail.com)*

<sup>b</sup>*Inorganic Materials and Catalysis Division, CSIR-Central Salt & Marine Chemicals Research Institute, G. B. Marg, Bhavnagar-364002, Gujarat, India.*

*E-mail: [ankush@csmcri.res.in](mailto:ankush@csmcri.res.in); [krishkicha545@gmail.com](mailto:krishkicha545@gmail.com)*

<sup>c</sup>*Academy of Scientific and Innovative Research (AcSIR), Ghaziabad-201002, India.*

<sup>‡</sup>*Contributed equally*

## Contents

Sr. No	Content	Page No.
1	Materials & Methods	S3
2	Controlled Experiments	S4
3	Studies on the variation of catalysts for the nitroaldol condensation between benzaldehyde and nitromethane	S5
3	The EDX analysis spectrum and mapping of the synthesized DFNS material (Fig. S1)	S6
4	The EDX analysis spectrum and the XPS analysis of the synthesized DFNS@NH <sub>2</sub> & the final Material DFNS@TBAB (Fig. S2-S3)	S7
5	The UV-Vis, Raman profiles, the Basicity profile, and the effect of time (Fig. S4-S6)	S8-9
6	Recyclability studies, the FeSEM & TEM images of the recycled catalyst (Fig. S7-8)	S9-10
7	Fig. S9 GC-MS profile for (2-nitrovinyl)benzene	S10-14
8	Fig. S10 GC-MS profile for 4-(2-nitrovinyl)phenol	
9	Fig. S11 GC-MS profile for 4-(1,3-dinitropropan-2-yl)phenol	
10	Fig. S12 GC-MS profile for 2-methoxy-4-(2-nitrovinyl)phenol	
11	Fig. S13 GC-MS profile for 4-(1,3-dinitropropan-2-yl)-2-methoxyphenol	
12	Fig. S14 GC-MS profile for 2-(2-nitrovinyl)benzene-1,3,5-triol	
13	Fig. S15 GC-MS profile for 2-(2-nitrovinyl)benzene-1,3,5-triol	
14	Fig. S16 GC-MS profile for 2-(2-nitrovinyl)phenol	
15	Fig. S17 GC-MS profile for 1-nitro-2-(2-nitrovinyl)benzene	
16	Fig. S18 GC-MS profile for 2-(2-nitrovinyl)furan	
17	Fig. S19 GC-MS profile for 2-methyl-5-(2-nitrovinyl)furan	
18	Fig. S20 GC-MS profile for (2-nitroprop-1-en-1-yl)benzene	
19	Fig. S21 GC-MS profile for 4-(2-nitroprop-1-en-1-yl)phenol	
20	Fig. S22 GC-MS profile for 2-methoxy-4-(2-nitroprop-1-en-1-yl)phenol	
21	Fig. S23 GC-MS profile for 1-nitro-2-(2-nitroprop-1-en-1-yl)benzene	
22	Fig. S24 GC-MS profile for 2-(2-nitroprop-1-en-1-yl)furan	
23	Fig. S25 GC-MS profile for 2-methyl-5-(2-nitroprop-1-en-1-yl)furan	
24	Fig. S26 GC-MS profile for 4-phenyl-1,3-dioxolan-2-one	
25	<sup>1</sup> H NMR & <sup>13</sup> C NMR spectrum of 2-methyl-5-(2-nitrovinyl)furan	S15
26	<sup>1</sup> H NMR & <sup>13</sup> C spectrum of 4-(2-nitrovinyl)phenol	S16
27	<sup>13</sup> C NMR spectrum of 2-methoxy-4-(2-nitrovinyl)phenol	S17
28	CO <sub>2</sub> optimization studies (Table S2) & Comparison table for the metal-free Henry reaction between benzaldehyde and nitromethane (Table S3)	S17-19
29	Comparison table for the metal-free catalysts for the synthesis of styrene carbonate from styrene oxide and CO <sub>2</sub> (Table S4) & Supporting references	S19-20

## 1. Materials & Methods

Tetraphenylphosphonium bromide (TPPB), Urea, p-Xylene, Propanol, TEOS, Benzaldehyde (99%), 2,4,6-trihydroxy benzaldehyde (98%), Vanillin (>98%), Furfural (>98%), Styrene oxide (97%), 5-Methylfurfural (>98%) and 3-APTES were obtained from Merck (Sigma-Aldrich) & TCI India Pvt. Ltd.; p-hydroxybenzaldehyde (95%), ammonium nitrate, and Nitromethane (98%) were obtained from SRL Pvt. Ltd.; 2-Nitrobenzaldehyde (99%), Salicylaldehyde (98%), Nitroethane (98%), Dry toluene, and Dry acetonitrile were obtained from Spectrochem Pvt. Ltd. All chemicals and dry solvents were used without further purification.

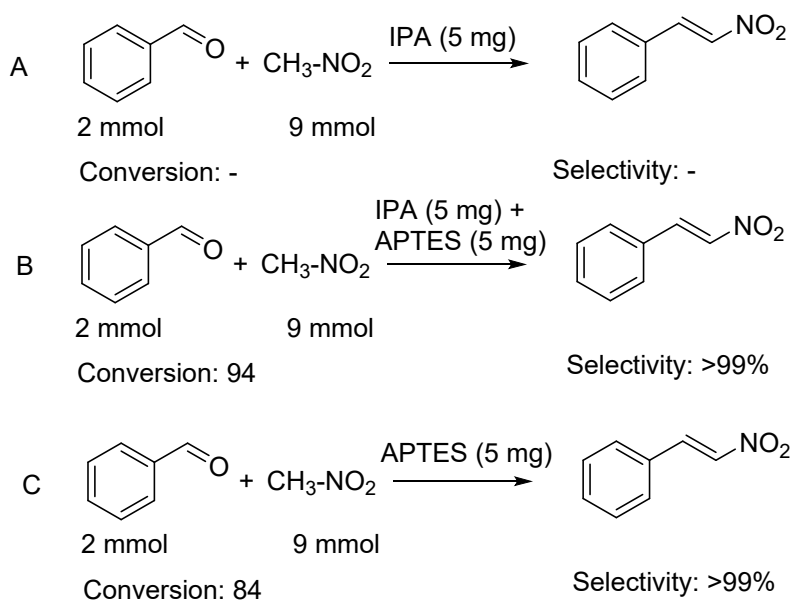
## 2. Instrumentation

For structural characterization, FTIR spectra were measured with a Perkin-Elmer GX spectrophotometer (manufactured in the USA) using KBr pellets. Surface area measurements were conducted with the Micromeritics 3 FLEX instrument, activating the sample at 65 °C for 50 minutes before analysis. Scanning electron microscopy (SEM-Leo series 1420 VP) equipped with INCA, and transmission electron microscopy (TEM) using a JEOL JEM 2100 microscope with Lacey carbon-coated grids, were employed to determine surface morphology. X-ray photoelectron spectroscopy (XPS) was conducted for chemical and surface state analysis using a Thermo Fisher Nexsa spectrophotometer with monochromated Al K $\alpha$  radiation (energy of 1486.6 eV). Powder X-ray diffraction profiles were recorded using a MiniFlex-II (FD 41521) powder diffractometer from Rigaku, Japan, with a scan rate of 1° per minute. Thermal stability investigation involved TGA analysis using a Mettler-Toledo (TGA/SDTA 851E) instrument in the presence of air, with a heating rate of 10 °C/min. Thermal stability was investigated using TGA analysis on a Mettler-Toledo (TGA/SDTA 851E) instrument in an air

atmosphere, with a heating rate of 10 °C/min. <sup>1</sup>H and <sup>13</sup>C NMR spectra were recorded on a Bruker Advance 500 MHz NMR. Thermal stability was investigated using TGA analysis on a Mettler-Toledo (TGA/SDTA 851E) instrument in an air atmosphere, with a heating rate of 10 °C/min. The conversion and selectivity were analysed using a gas chromatography system equipped with an FID detector (GC-7890B-Agilent) with HP-5 column, consisting of 5% diphenyl and 95 % dimethyl polysiloxane capillary stationary phase and nitrogen as the carrier gas. The product was confirmed by GC-MS (equipped with FID as a detector (GC-MS Shimadzu, QP-2010, Japan) with HP-5 column which consists of 5 % diphenyl and 95 % dimethyl polysiloxane capillary phase with helium as the carrier gas and NMR analysis.

### 3. Controlled Experiments

IPA (-OH) and APTMS (-NH<sub>2</sub>) were taken as model compounds for the amine and hydroxyl functionality of DFNS@NH<sub>2</sub> (**Scheme S1**). The presence of Si-OH and -NH<sub>2</sub> from DFNS@NH<sub>2</sub> was confirmed by FT-IR.



**(Scheme S1): Reaction Conditions:** Benzaldehyde: 2 mmol, Nitromethane: 11.2 mmol, Temperature; 50 °C, 6 h, Catalyst; 5 mg, A-IPA (5 mg), B-IPA+APTES (5+5 mg), and C-IPA (5 mg).

**Table S1.** Studies on the variation of catalysts for the nitroaldol condensation between benzaldehyde and nitromethane

Entry	Catalyst	Conv. (%)	Selectivity (%)	
			B	C
1	blank	-	-	-
2	Si(OH) <sub>4</sub>	-	-	-
3	SiO <sub>2</sub>	-	-	-
4	SiO <sub>2</sub> @NH <sub>2</sub>	3	100	-
5	Ba(OH) <sub>2</sub>	-	-	-
6	DFNS@NH <sub>2</sub>	>87	>99	-
7	MgO	51	>99	-
8	MgO-NH <sub>2</sub>	>99	89	11

<sup>a</sup>**Reaction condition:** Benzaldehyde: 2 mmol (0.2 ml), Nitromethane: 9 mmol (0.6 ml), Temperature; 50 °C, 6 h

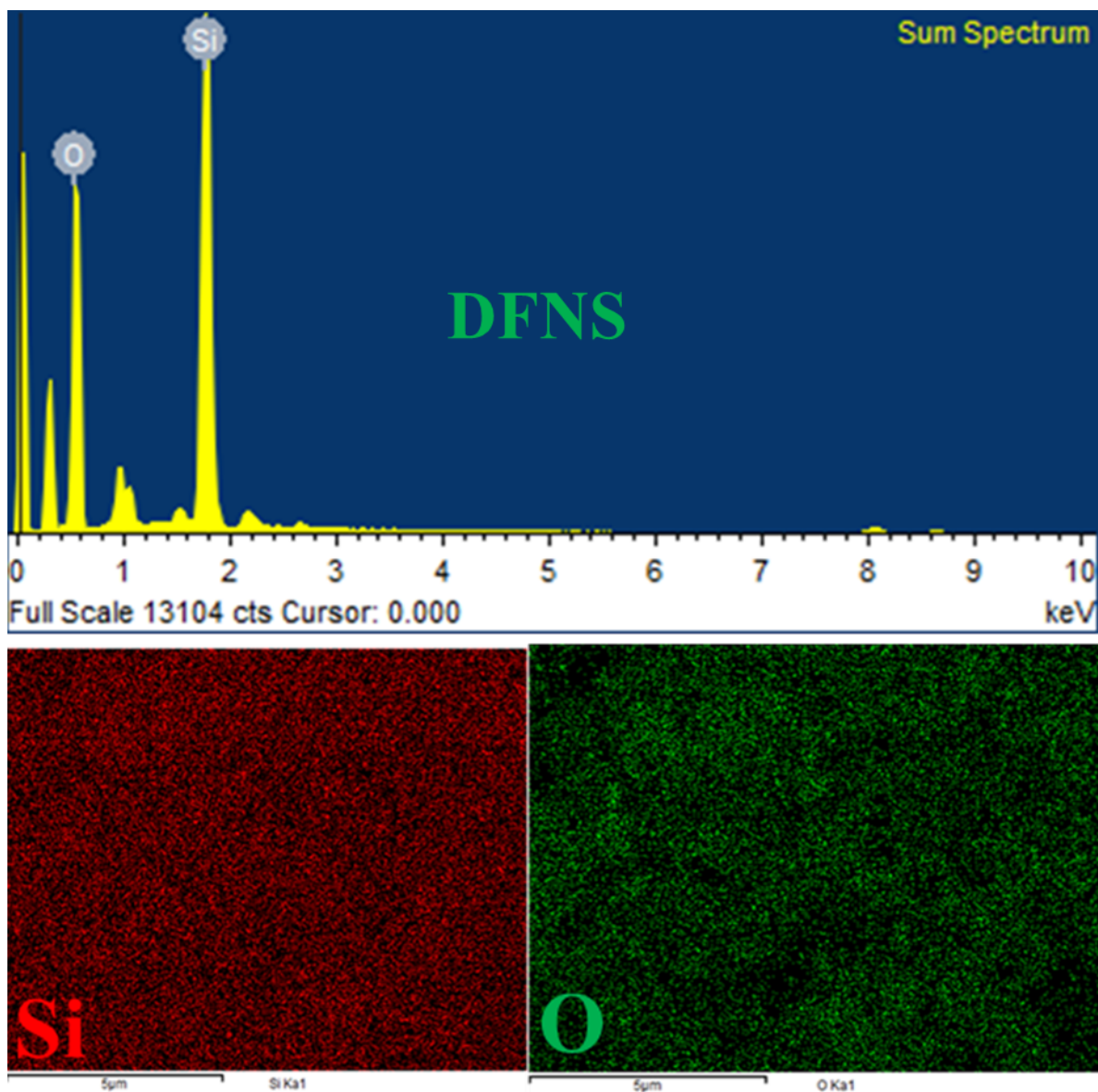


**Fig. S1** The EDX analysis spectrum and mapping of the synthesized DFNS material.

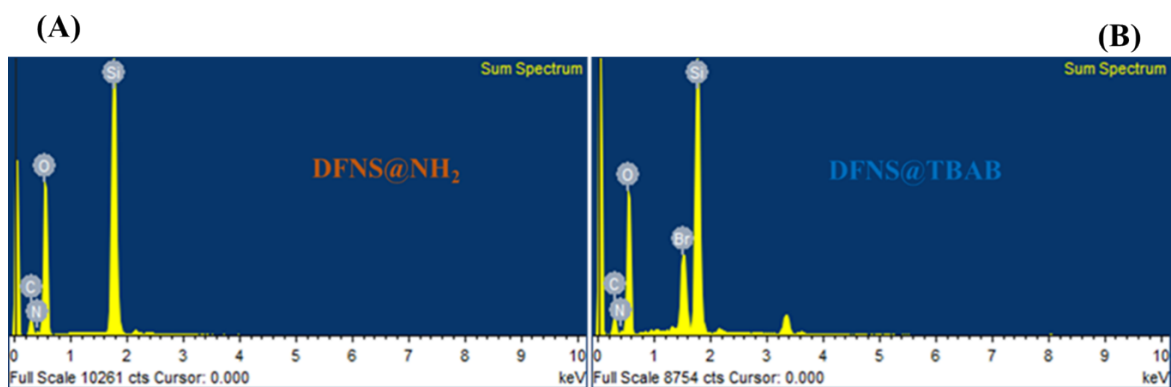


**Fig. S2** (A) The EDX analysis spectrum of the synthesized DFNS@NH<sub>2</sub> & the final Material DFNS@TBAB (B).

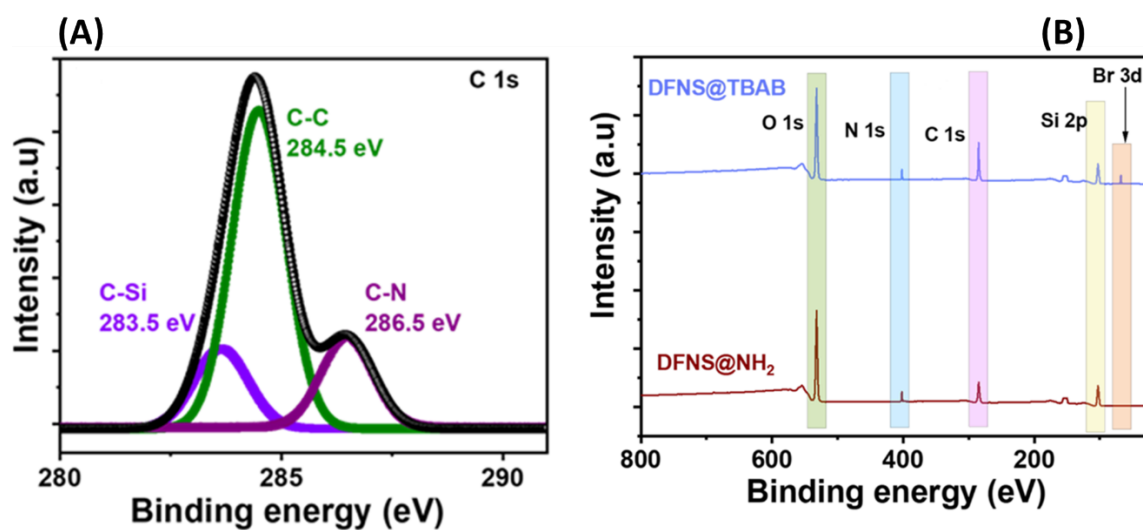


**Fig. S3** (A, B) The comparison of the XPS spectrum of the synthesized DFNS@NH<sub>2</sub> & the final material DFNS@TBAB.

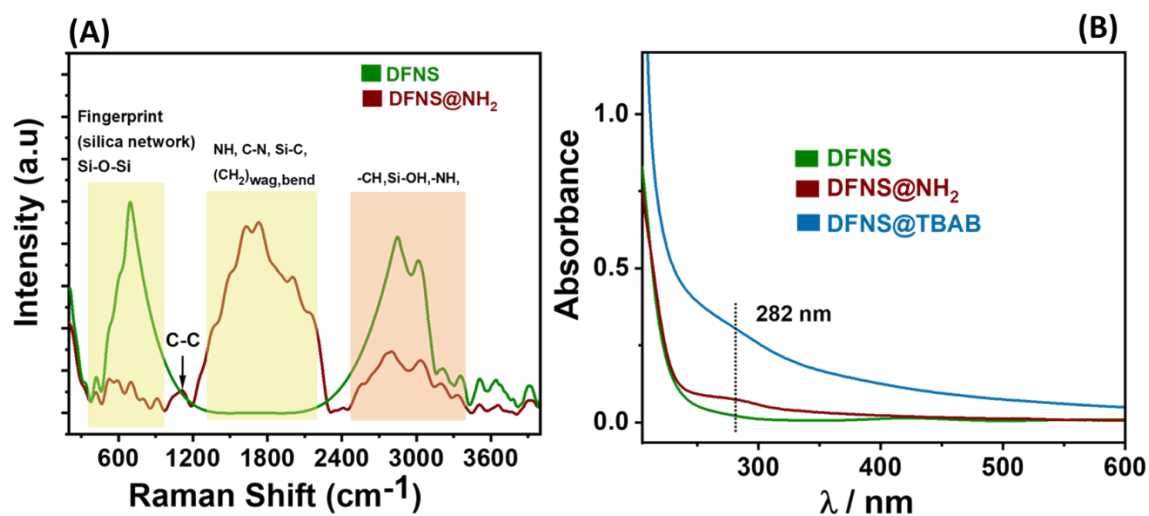


**Fig. S4** (A) The comparison of the Raman spectra of the synthesized DFNS and aminated DFNS@NH<sub>2</sub> materials; (B) The UV-Vis profile of the DFNS, DFNS@NH<sub>2</sub> & DFNS@TBAB materials

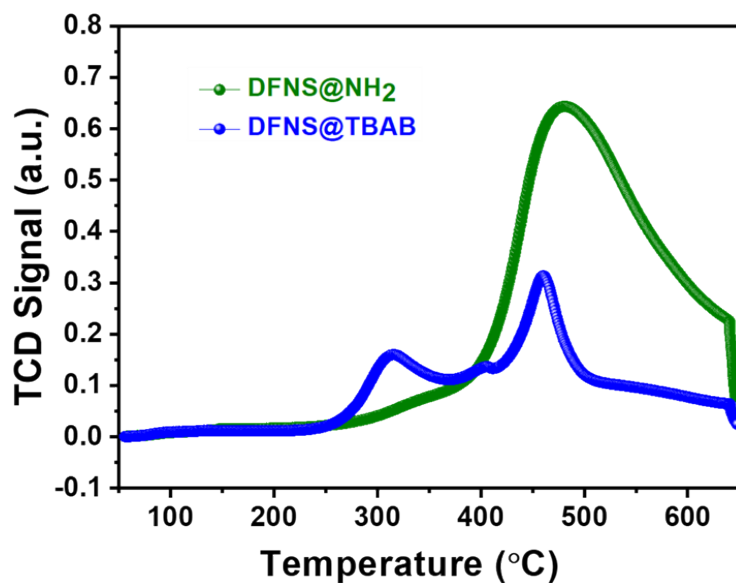


**Fig. S5** The CO<sub>2</sub>-TPD of DFNS@NH<sub>2</sub> and DFNS@TBAB.



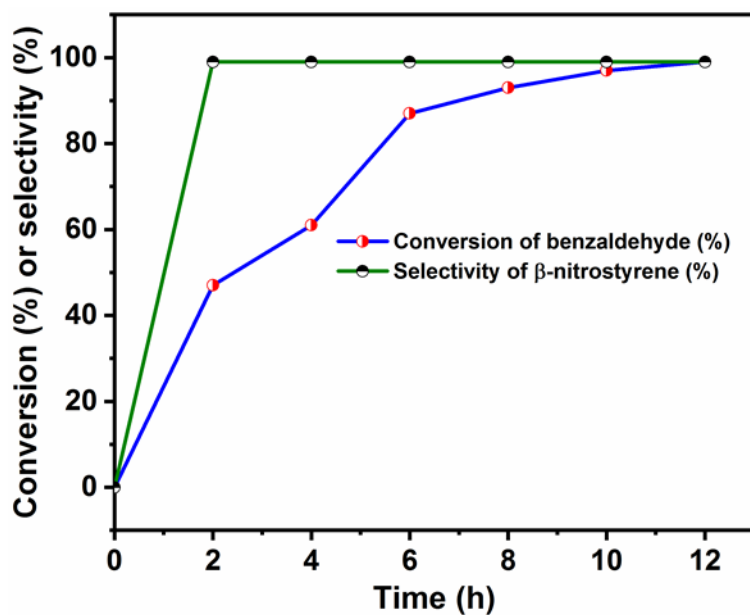


**Fig. S6** Effect of time, Reaction condition: Benzaldehyde; 2 mmol, Nitromethane; 11.2 mmol, Catalyst; 20 mg, Temperature; 50 °C.

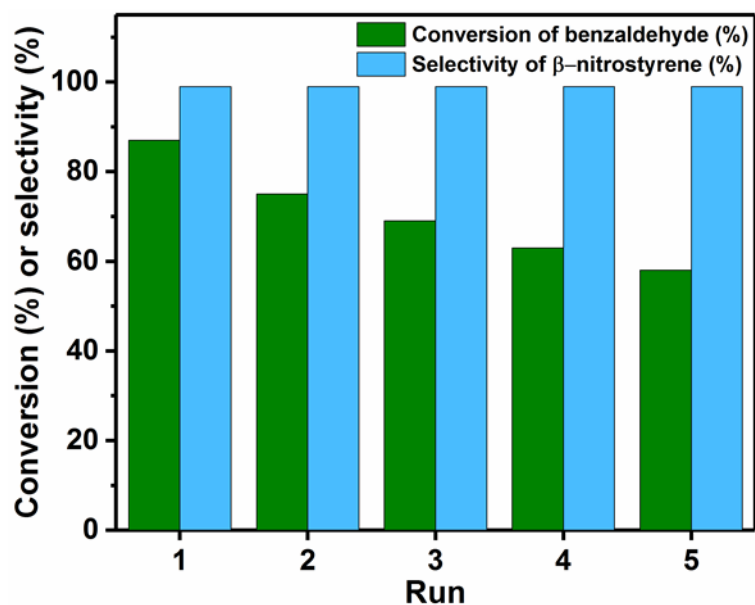


**Fig. S7** Recyclability studies of DFNS@NH<sub>2</sub><sup>a</sup> Reaction condition: Benzaldehyde: 2 mmol, Nitroethane: 11.2 mmol, Catalyst 20 mg, Temperature; 50°C, Time: 6 h.

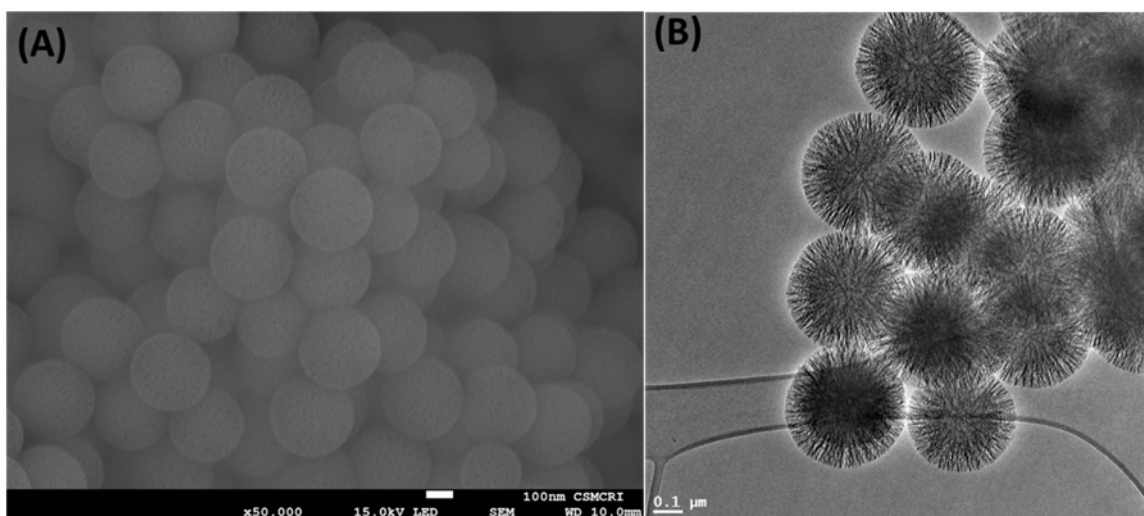


**Fig. S8** (A, B) The FeSEM and TEM images of the recycled catalyst after 5 cycles having retained dendritic morphology.

#### 4. GC-MS profile of the selected products

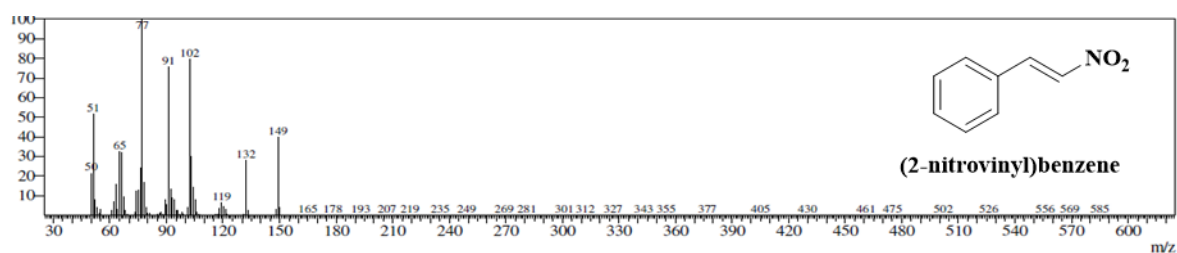


**Fig. S9** GC-MS profile for (2-nitrovinyl)benzene.

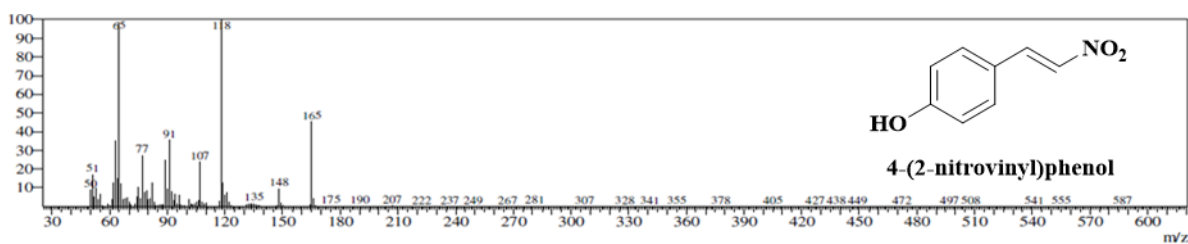


Fig. S10 GC-MS profile for 4-(2-nitrovinyl)phenol.

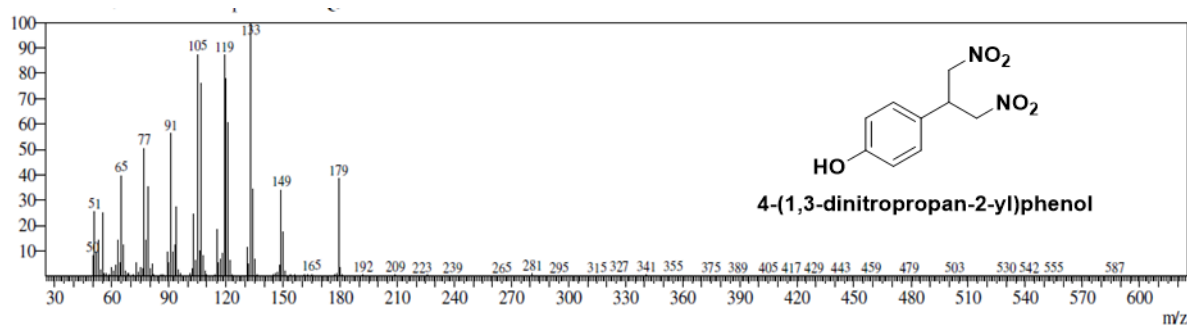


Fig. S11 GC-MS profile for 4-(1,3-dinitropropan-2-yl)phenol.

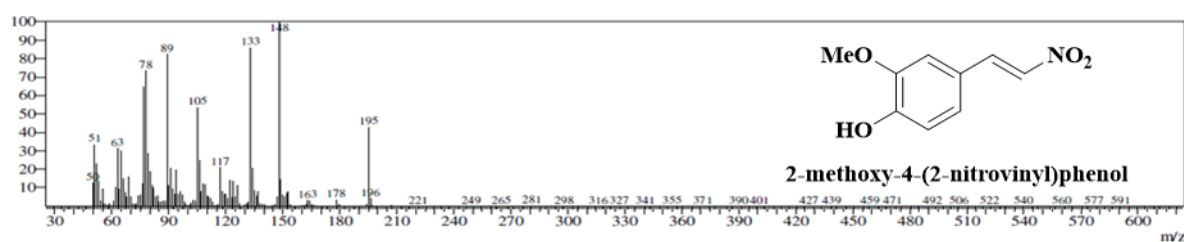


Fig. S12 GC-MS profile for 2-methoxy-4-(2-nitrovinyl)phenol.

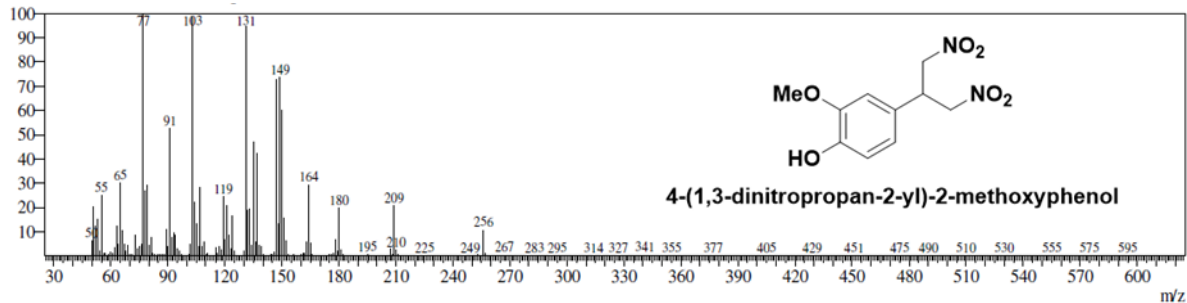


Fig. S13 GC-MS profile for 4-(1,3-dinitropropan-2-yl)-2-methoxyphenol.

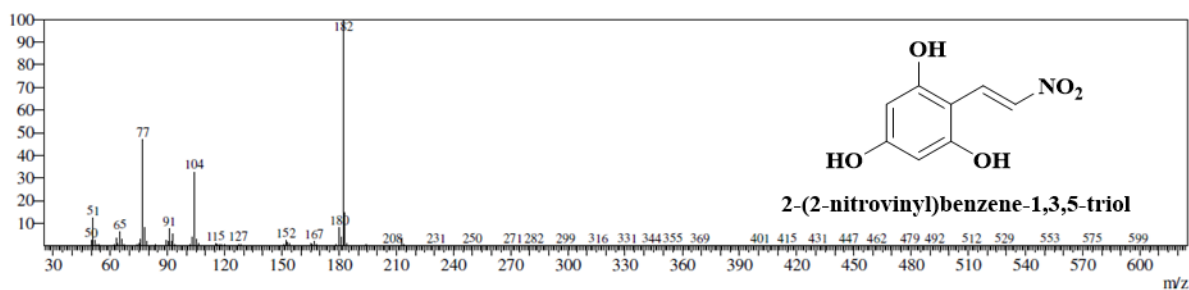


Fig. S14 GC-MS profile for 2-(2-nitrovinyl)benzene-1,3,5-triol.

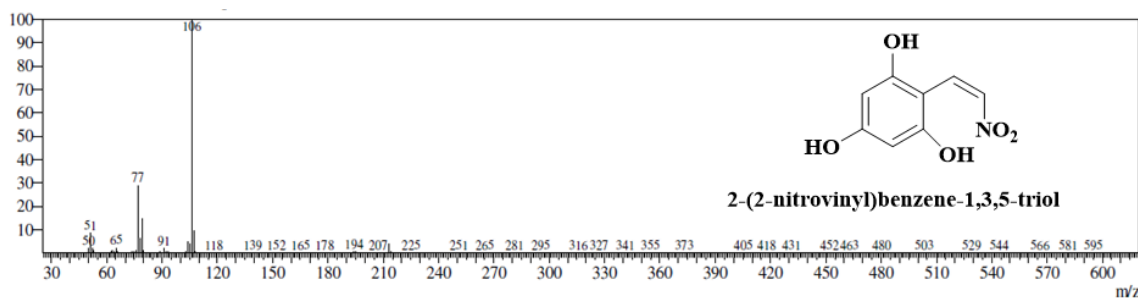


Fig. S15 GC-MS profile for 2-(2-nitrovinyl)benzene-1,3,5-triol.

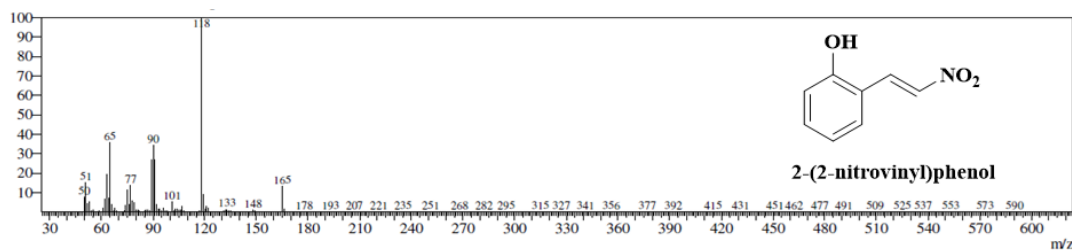


Fig. S16 GC-MS profile for 2-(2-nitrovinyl)phenol.

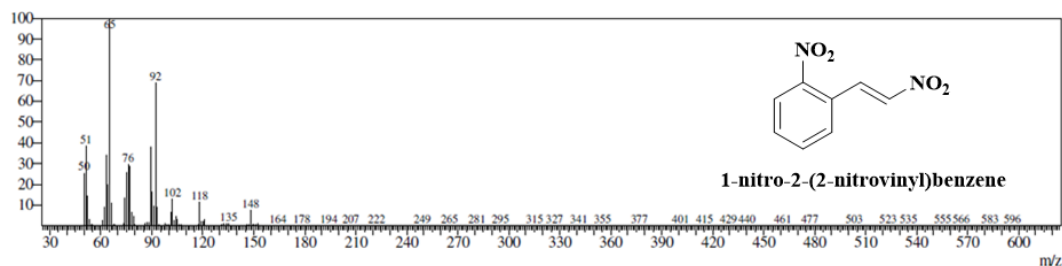


Fig. S17 GC-MS profile for 1-nitro-2-(2-nitrovinyl)benzene.

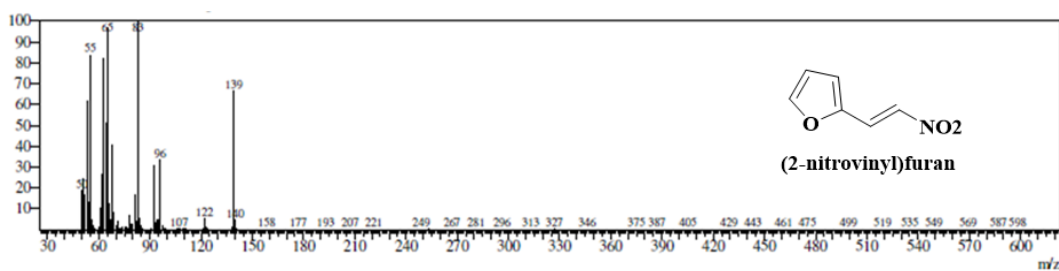
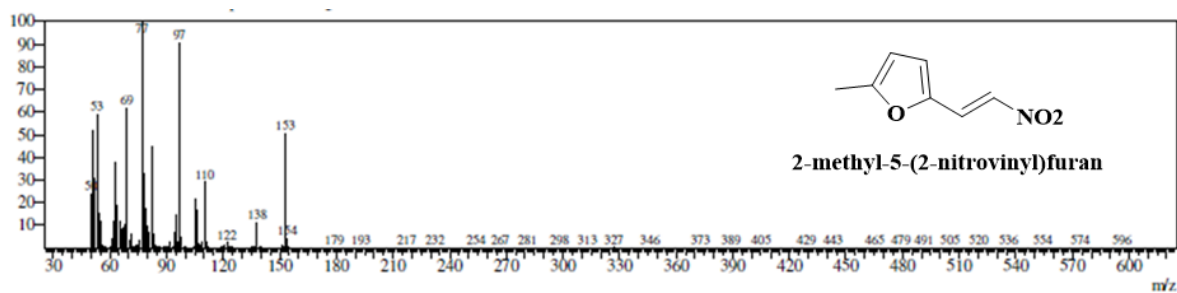
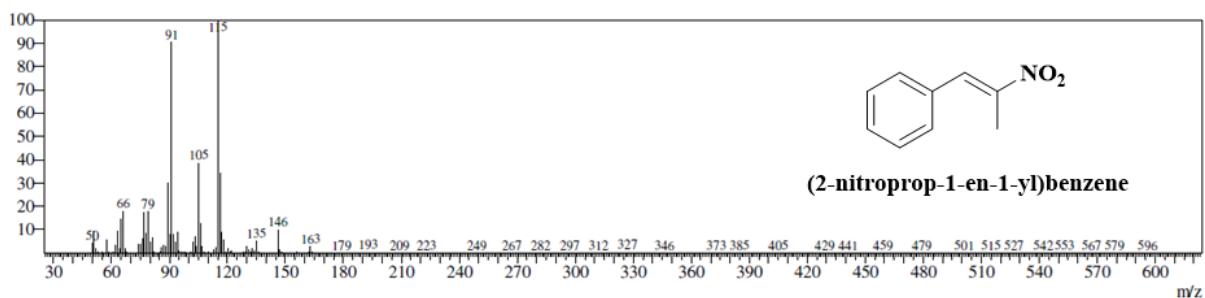


Fig. S18 GC-MS profile for 2-(2-nitrovinyl)furan.



**Fig. S19** GC-MS profile for 2-methyl-5-(2-nitrovinyl)furan.



**Fig. S20** GC-MS profile for (2-nitroprop-1-en-1-yl)benzene.

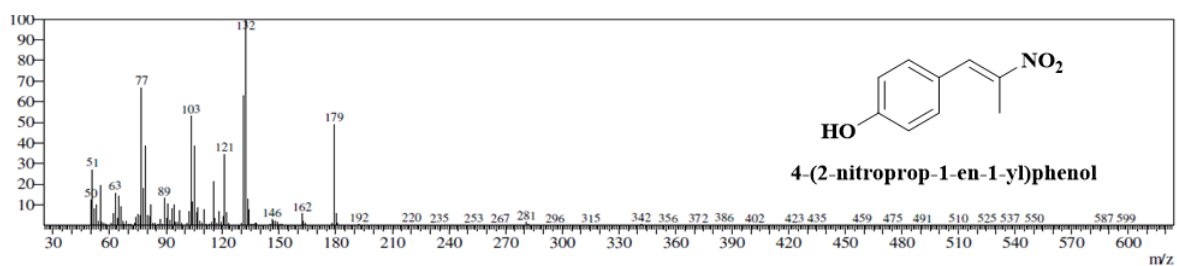


**Fig. S21** GC-MS profile for 4-(2-nitroprop-1-en-1-yl)phenol.

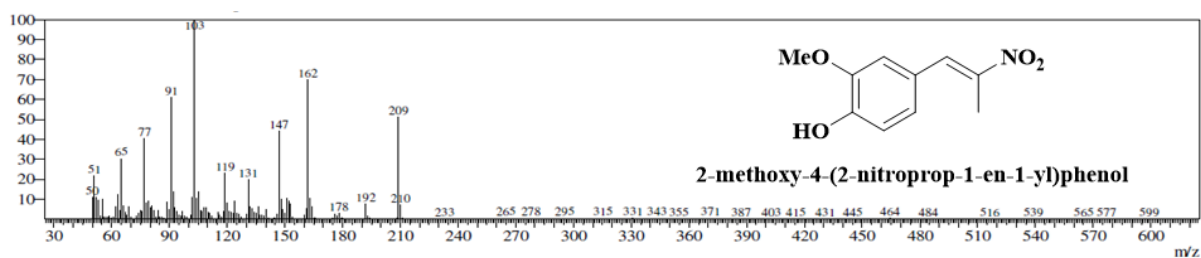


**Fig. S22** GC-MS profile for 2-methoxy-4-(2-nitroprop-1-en-1-yl)phenol.

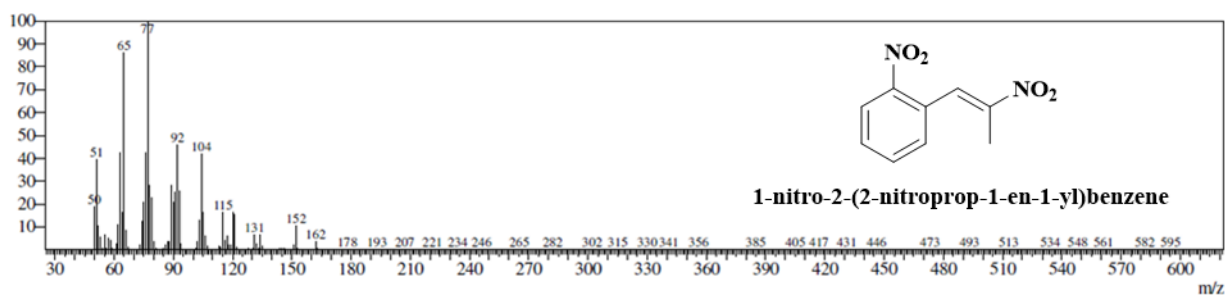


**Fig. S23** GC-MS profile for 1-nitro-2-(2-nitroprop-1-en-1-yl)benzene.

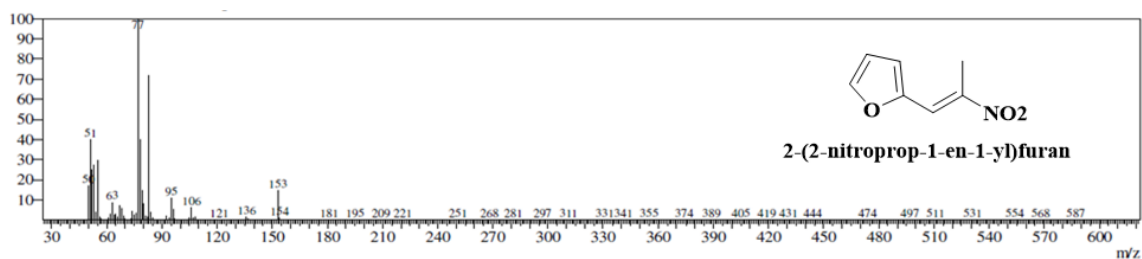


**Fig. S24** GC-MS profile for 2-(2-nitroprop-1-en-1-yl)furan.

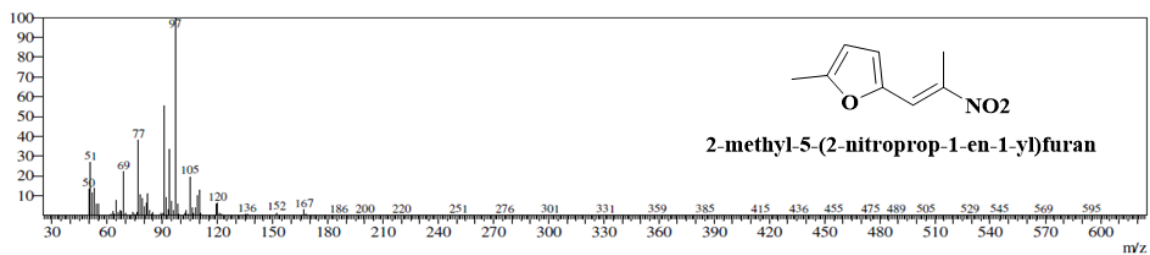


**Fig. S25** GC-MS profile for 2-methyl-5-(2-nitroprop-1-en-1-yl)furan.

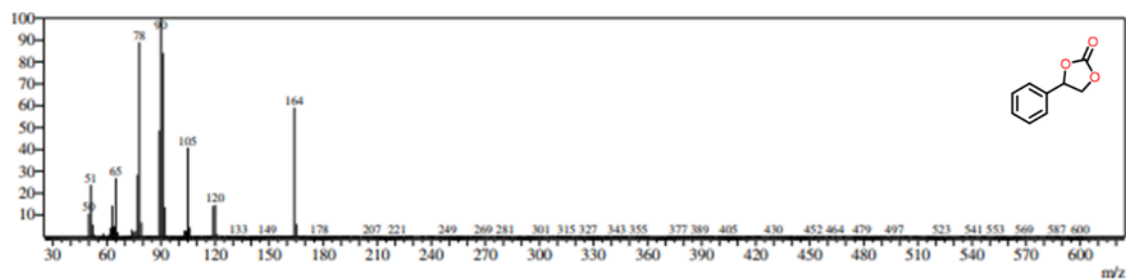


**Fig. S26** GC-MS profile for 4-phenyl-1,3-dioxolan-2-one

**5.  $^1\text{H}$  and  $^{13}\text{C}$  NMR analysis**

$^1\text{H}$  and  $^{13}\text{C}$  NMR analysis

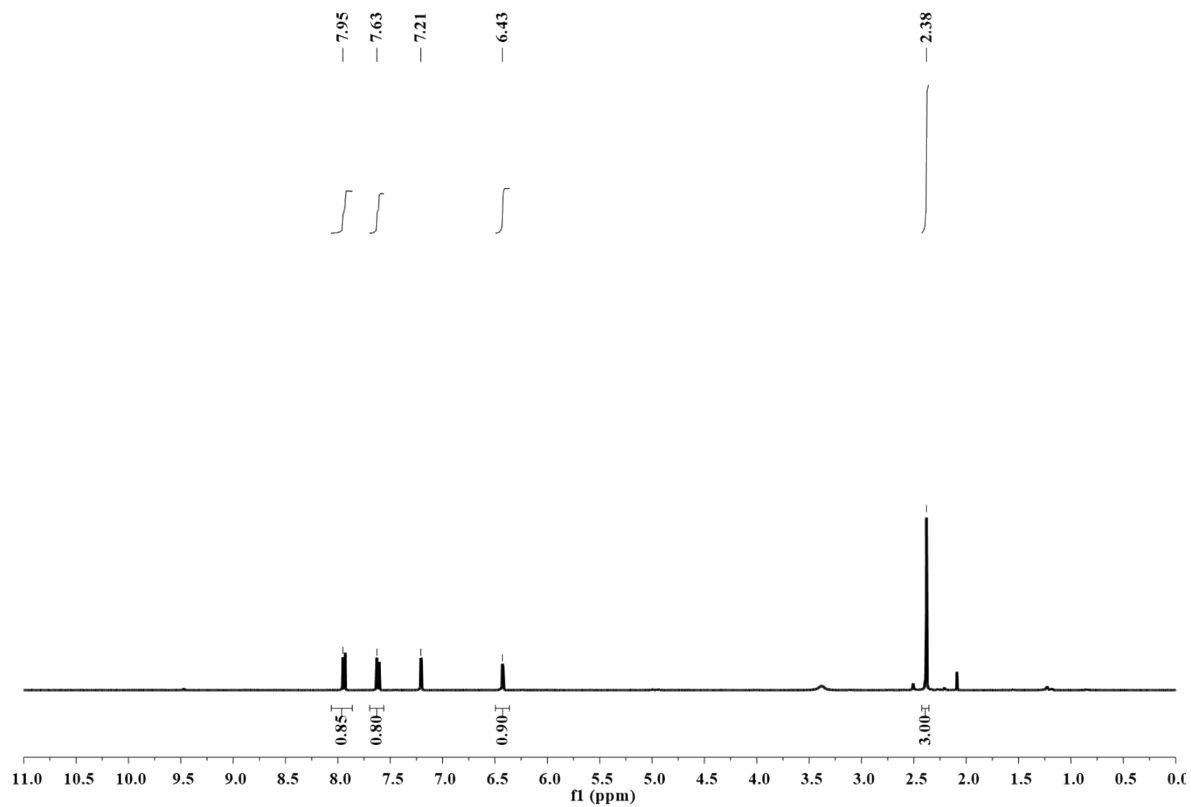


**Fig. S27**  $^{13}\text{C}$  NMR spectrum of 2-methyl-5-(2-nitrovinyl)furan

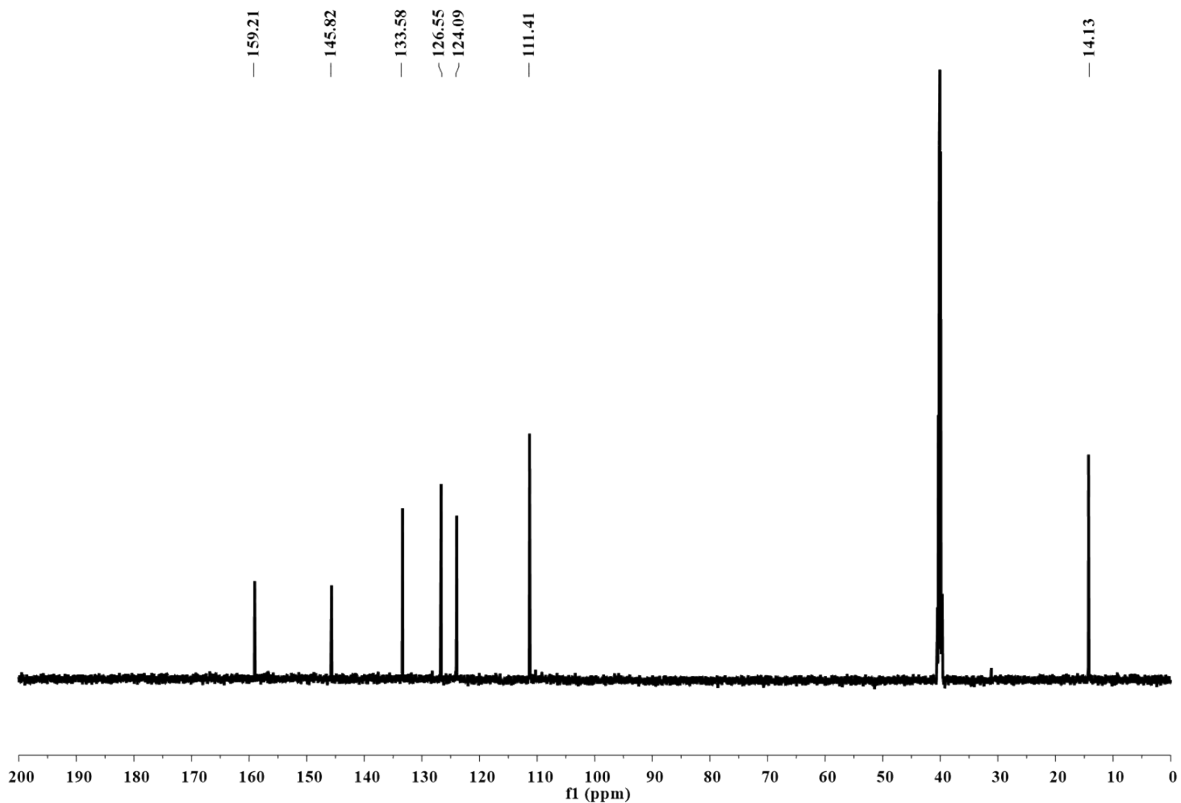


**Fig. S28**  $^{13}\text{C}$  NMR spectrum of 2-methyl-5-(2-nitrovinyl)furan

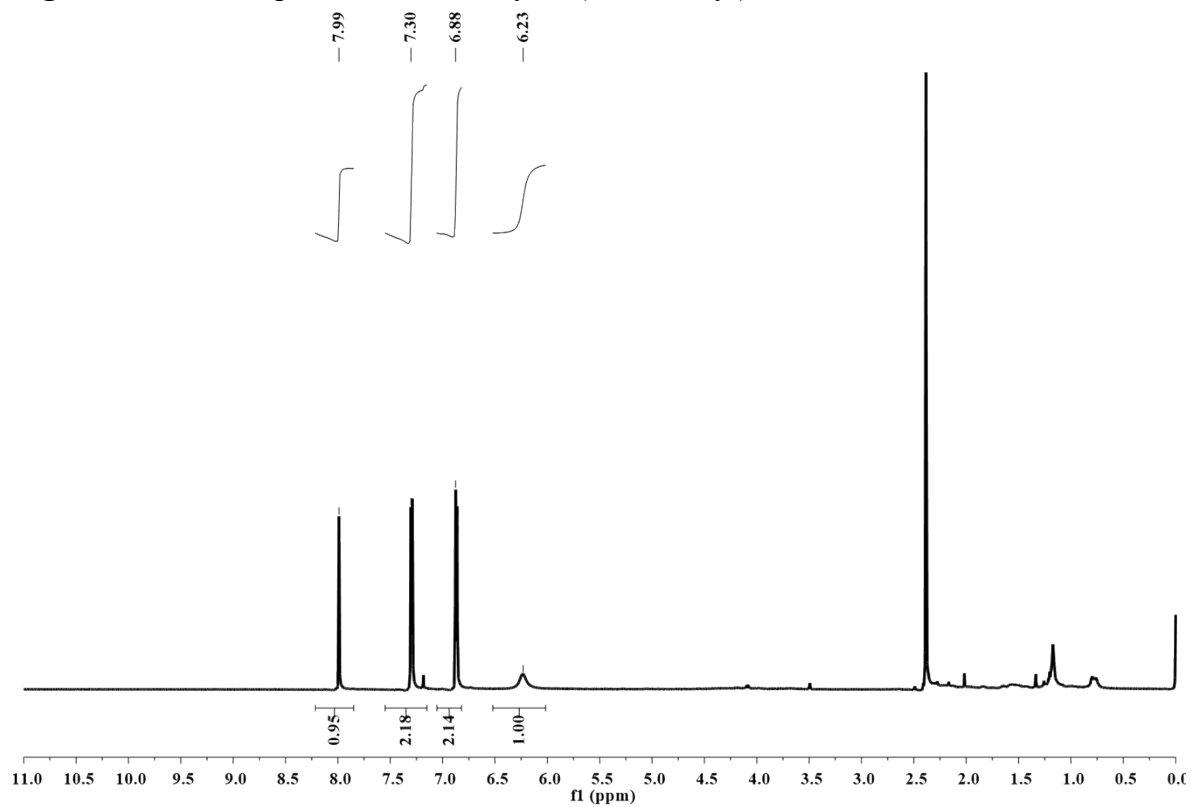


**Fig. S29**  $^1\text{H}$  NMR spectrum of 4-(2-nitrovinyl)phenol

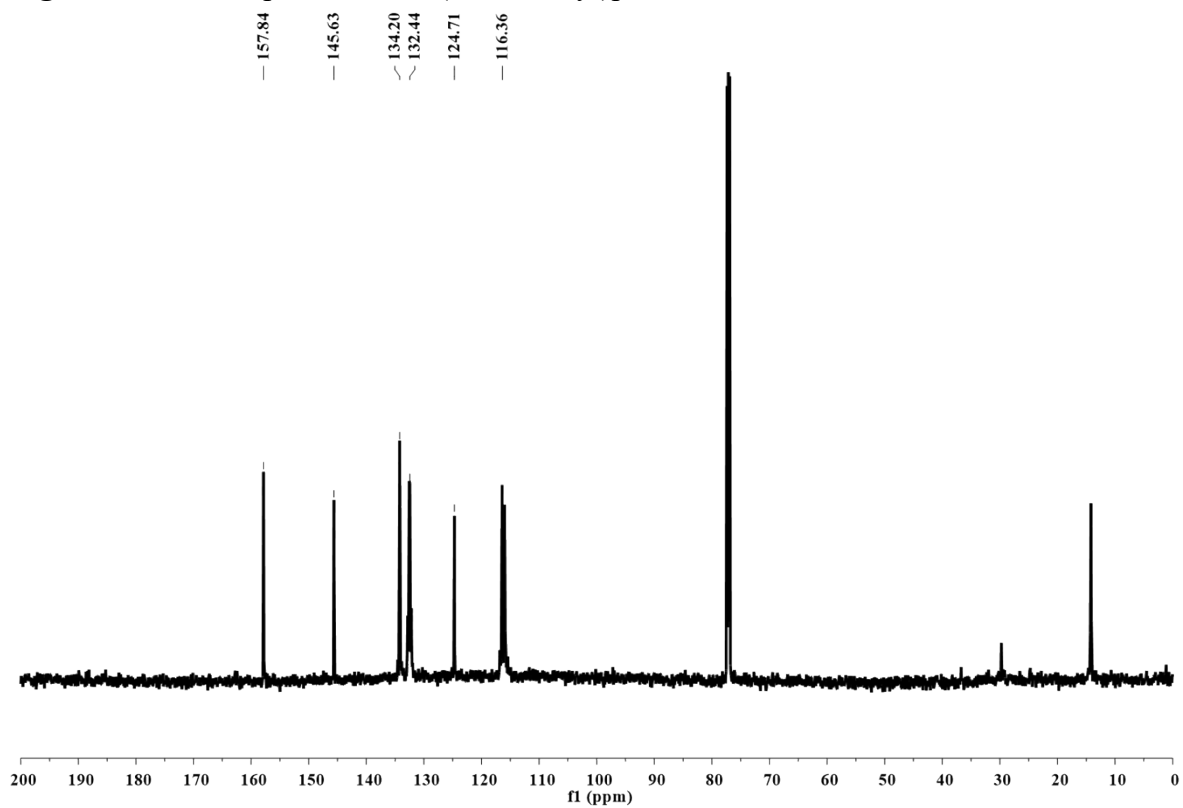


**Fig. S30**  $^{13}\text{C}$  NMR spectrum of 4-(2-nitrovinyl)phenol



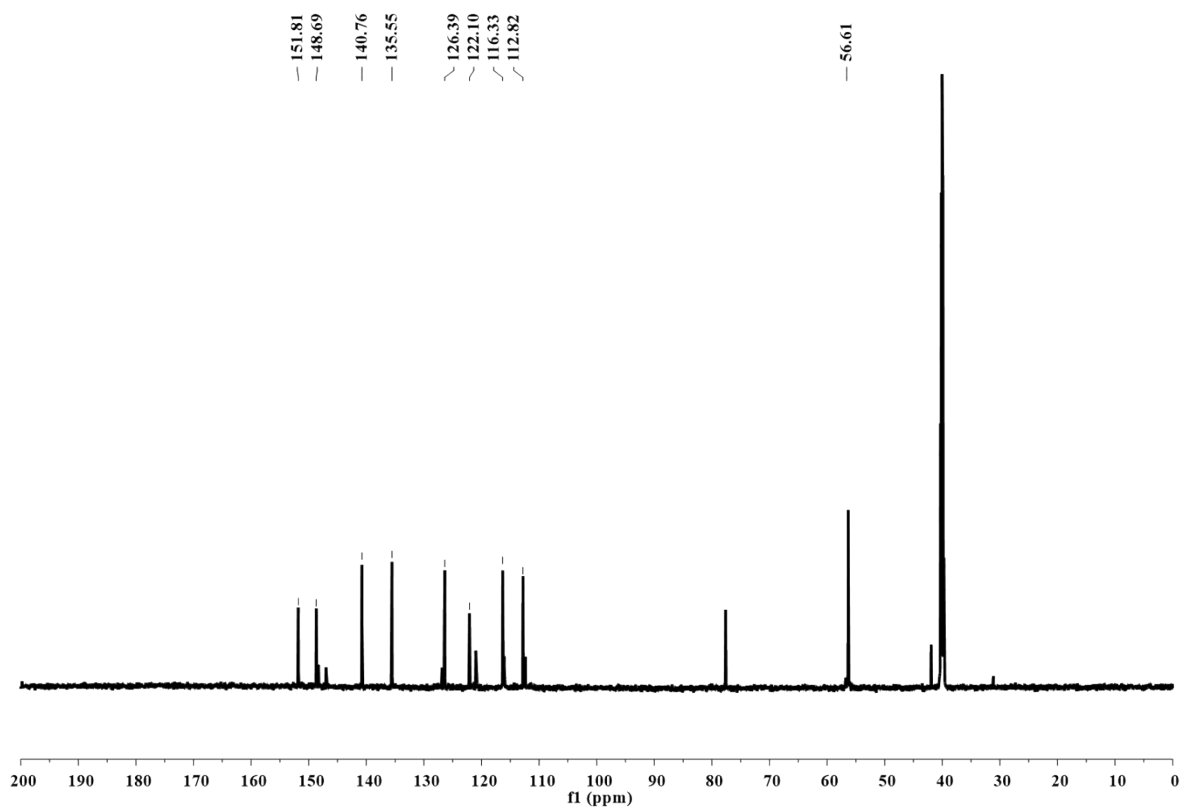


**Fig. S31**  $^{13}\text{C}$  NMR spectrum of 2-methoxy-4-(2-nitrovinyl)phenol

Table S2. Optimization studies cycloaddition of styrene oxide with  $\text{CO}_2$  using DFNS@TBAB

Entry	Catalyst	Catalyst amount	Temp ( $^{\circ}\text{C}$ )	Time (h)	Conv. (%)	Sel. (%)
1	-	-	100	12	-	-
2	DFNS@ $\text{NH}_2$	25	100	12	-	-
3 <sup>a</sup>	DFNS@ $\text{NH}_2$ + CTAB	25	100	12	96	90
4 <sup>b</sup>	DFNS@ $\text{NH}_2$ + KI	25	100	12	90	88
5 <sup>c</sup>	DFNS@ $\text{NH}_2$ + n-BB	25	100	12	46	94
6 <sup>d</sup>	n-BB	25	100	12	16	90
7	DFNS@TBAB	25	100	12	34	90
8	DFNS@TBAB	12.5	100	12	14	93
9	DFNS@TBAB	50	100	12	58	98
10	DFNS@TBAB	50	100	12	72	98
11	DFNS@TBAB	100	100	12	100	98

12	DFNS@TBAB	25	60	12	-	-
13	DFNS@TBAB	25	80	12	10	98
14	DFNS@TBAB	25	100	12	36	98
15	DFNS@TBAB	25	120	12	88	98
16	DFNS@TBAB	25	120	3	10	98
17	DFNS@TBAB	25	120	6	34	98
18	DFNS@TBAB	25	120	9	66	98
19	DFNS@TBAB	25	120	12	88	98
20	DFNS@TBAB	25	120	15	94	98

Reaction conditions: Styrene oxide: 2.08 mmol and balloon CO<sub>2</sub> pressure, <sup>(a)</sup>CTAB (5 mg), <sup>(a)</sup>KI (5 mg), <sup>(c)</sup>n-BB (5 mg), and <sup>(d)</sup>25 mg. n-BB: n-butyl bromide

**Table S3.** Comparison of metal-free catalyst for Henry reaction between benzaldehyde and nitromethane

Sr. No.	Catalyst	Reaction condition	Yield (%)	Reference
1	$\mu$ -Chlorotris(tetrahydrofuran)[tris[1,1,1-trimethyl- <i>N</i> -(trimethylsilyl)silanaminat	Catalyst: 2 mol%, BA: 1 equivalent, NM: 1 equivalent, THF, 66 °C, 24 h	10	S1
2	Ammonium acetate	Catalyst: 0.3 mmol, BA: 1 mmol, NM: 3 mL, microwave, 90 °C, 1 h	95	S2
3	Amine functionalized Yolk-shell-structured mesoporous silica	Catalyst: 5 mol%, BA: 1.0 mmol, NM: 1.0 mL, 90 °C, 3 h	99	S3
4	SiO <sub>2</sub> and triethylamine	Catalyst: 200 mg, Triethylamine: 0.2 mmol, BA: 2.0 mmol, NM: 2 mL, 50 °C, 17 h	18	S4
5	AFB	Catalyst: 26.5 mg, BA: 2.5 mmol, NM: 2 mL, 90 °C, 6 h	92	S5

6	AP-GO	Catalyst containing 0.075 mmol nitrogen species, BA: 0.306 mL (3.0 mmol), NM: 6.0 mL, 100 °C, 6.0 h	90	S6
7	DFNS@NH <sub>2</sub>	Catalyst: 20 mg, BA: 2 mmol, NM: 11.2 mmol, , 60 °C, 6 h,	>99	<b>This work</b>

BA: Benzaldehyde, NM: Nitromethane, AP-GO: Graphene oxide-supported primary amine, AFB: Amine functionalized bagasse

**Table S4.** Comparison of metal-free catalysts for the synthesis of styrene carbonate from styrene oxide and CO<sub>2</sub>

Catalyst	Co-catalyst	Reaction conditions	Conv. (%)	Sel. (%)	Ref.
SB	KI	2 MPA CO <sub>2</sub> , 120 °C, 6 h	87	99	S7
COP-222	-	0.1 MPA CO <sub>2</sub> , 100 °C, 24 h	99	99	S8
Amb-OH-I-910	-	3.0 MPa of CO <sub>2</sub> , 120 °C, 24 h	-	99	S9
PQPBrCO OH	-	0.1 MPA CO <sub>2</sub> , 120 °C, 12 h	-	98.2	S10
CSGOArg aerogels	THAB	100 °C, 8 h	-	65.39 <sup>a</sup>	S11
[CMPy]Br/MA (1:1)	-	CO <sub>2</sub> balloon pressure, 90 °C, 1 h	100	100	S12
[TMGVBr]10@COF	-	0.1 MPA CO <sub>2</sub> , acetonitrile (2 mL), 100 °C, 10 h	-	41.7 <sup>a</sup>	S13
Ketimine derivatives	TBAI	1 MPA CO <sub>2</sub> , RT, 24 h	-	94 <sup>a</sup>	S14
QAFB	-	0.1 MPA CO <sub>2</sub> , 120 °C, 12 h	61	99	S5
<b>DFNS@T</b>	-	<b>CO<sub>2</sub> (balloon pressure),</b>	<b>94</b>	<b>98</b>	<b>This</b>

---

**Abbreviations:** SO: Styrene oxide, C<sub>3</sub>N<sub>4</sub>: Graphitic carbon nitride, u-g-C<sub>3</sub>N<sub>4</sub>: Urea derived graphitic carbon nitride, p-TBIB: metal-free microporous polymeric spheres catalyst, P-g-C<sub>3</sub>N<sub>4</sub>: Phosphorus doped graphitic carbon nitride, Amb-OH-I-910: Ion-exchange step into their iodide counterparts, OX-BC: Oxidised biochar, SB: sugarcane bagasse, QAFB: Quaternary ammonium salt functionalized sugarcane bagasse, tetrabutylammonium bromide (TBAB), [CMPy]Br: 1-(carboxymethyl)pyridinium bromide, KI: Potassium iodide.<sup>a</sup>Yield

---

## References

1. Y. Y. Liu, S. W. Wang, L. J. Zhang, Y. J. Wu, Q. H. Li, G. S. Yang, M. H. Xie, *Chin. J. Chem.*, 2008, **26**, 2267-2272.
2. J. M. Rodríguez, M. D. Pujol, *Tetrahedron Lett.*, 2011, **52**, 2629-2632.
3. J. An, T. Cheng, X. Xiong, L. Wu, B. Han, G. Liu, *Catal. Sci. Technol.*, 2016, **6**, 5714-5720.
4. K. Tanemura, T. Suzuki, *Tetrahedron Lett.*, 2018, **59**, 392-396.
5. K. Ravi, S. Mehra, S. Tothadi, A. Kumar, A. V. Biradar, *J. Environ. Chem. Eng.*, 2023, **11**, 109737.
6. F. Zhang, H. Jiang, X. Wu, Z. Mao, H. Li, *ACS Appl. Mater. Interfaces.*, 2015, **7**, 1669-1677.
7. W. Chen, L. X. Zhong, X. W. Peng, R. C. Sun, F. C. Lu, *ACS Sustain. Chem. Eng.*, 2015, **3**, 147-152.
8. S. Subramanian, J. Oppenheim, D. Kim, T. S. Nguyen, W. M. Silo, B. Kim, C. T. Yavuz, *Chem*, 2019, **5**, 3232-3242.
9. Y. A. Alassmy, Z. Asgar Pour, P. P. Pescarmona, *ACS Sustain. Chem. Eng.*, 2020, **8**, 7993-8003.
10. Y. L. Wan, Z. Zhang, C. Ding, L. Wen, *J. CO<sub>2</sub> Util.*, 2021, **52**, 101673.
11. Y. L. Wan, Z. Zhang, C. Ding, Wen, L. *J. CO<sub>2</sub> Util.*, 2022, **59**, 101958.
12. F. Norouzi, A. Abdolmaleki, *J. Environ. Chem. Eng.*, 2024, **12**, 111984.
13. Q. Xue, P. Wang, L. Cheng, Y. Wei, Y. Wang, J. Lin, G. Guan, Q. Xue, *Sep. Purif. Technol.*, 2025, **352**, 128175.
14. S. Roy, K. Das, S. Halder, *Catal. Lett.*, 2024, **154**, 2243-2254.